Supplement of

Multi-centennial climate change in a warming world beyond 2100

Sun-Seon Lee[1,2*], Sahil Sharma[1,2], Nan Rosenbloom[3], Keith B. Rodgers[4*], Ji-Eun Kim[1,2], Eun Young Kwon[1,2], Christian L.E. Franzke[1,2], In-Won Kim[1,2], M. G. Sreeush[5], and Karl Stein[1,2]

[1]Center for Climate Physics, Institute for Basic Science, Busan, Republic of Korea
[2]Pusan National University, Busan, Republic of Korea
[3]National Center for Atmospheric Research, Boulder, CO, USA
[4]WPI-Advanced Institute for Marine Ecosystem Change, Tohoku University, Sendai, Japan
[5]Alfred Wegener Institute, Helmholtz Centre for Polar and Marine Research, Am Handelshafen 12, 27570 Bremerhaven, Germany

Correspondence to: Sun-Seon Lee (sunseonlee@pusan.ac.kr) and Keith B. Rodgers (keith.rodgers.b2@tohoku.ac.jp)

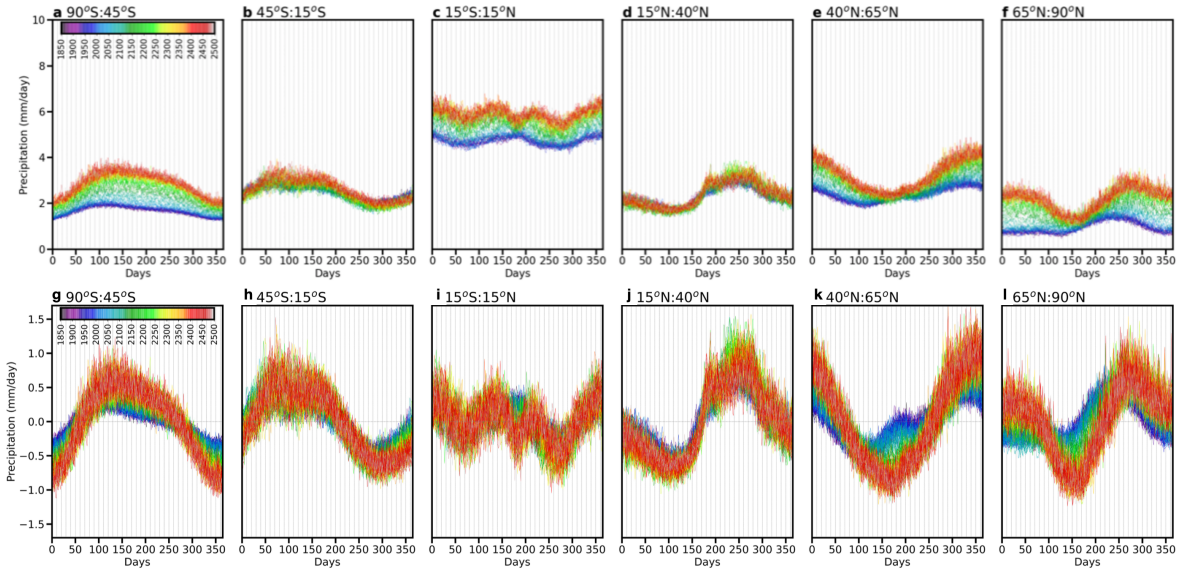

Figure S1: Seasonal cycle of daily precipitation (mm day^{-1}) along latitudinal bands. (a, g) 90°S-45°S, (b, h) 45°S-15°S, (c, i) 15°S-15°N, (d, j) 15°N-40°N, (e, k) 40°N-65°N, and (f, l) 65°N-90°N. Upper panels show daily mean precipitation in 5-year intervals and low panels show daily precipitation anomaly obtained by removing the annual mean from each year.

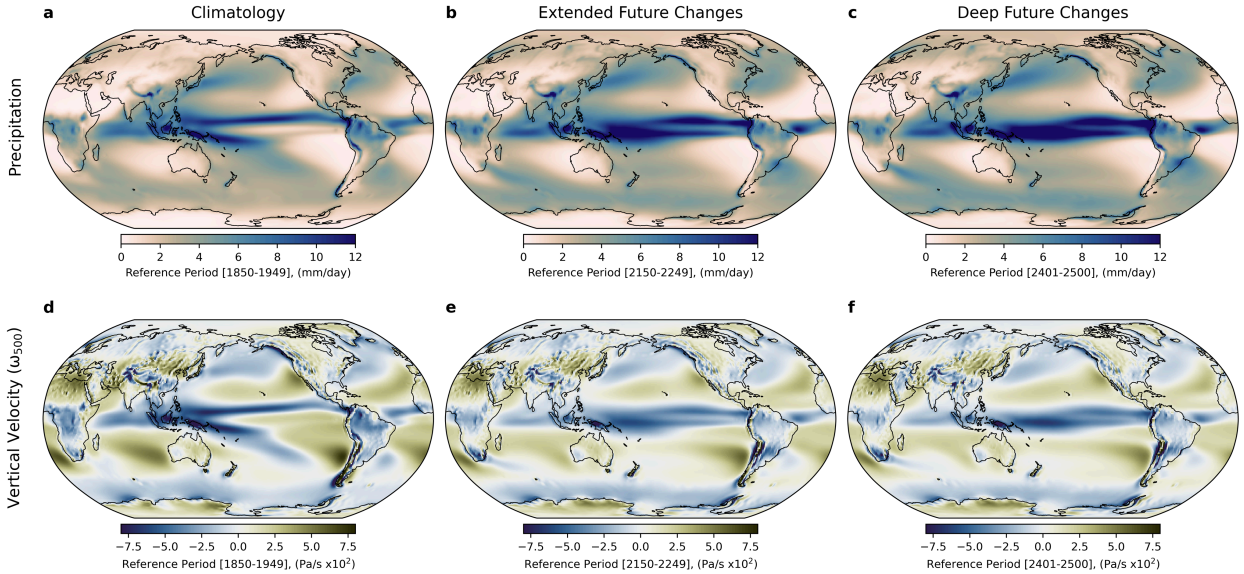

Figure S2: Reference climatology of precipitation (mm day^{-1}; upper panels) and 500 hPa vertical p-velocity (Pa s^{-1} x 10^2; lower panels). (a, d) Period spanning 1850-1949, (b, e) period spanning 2150-2249, and (c, f) period spanning 2401-2500.

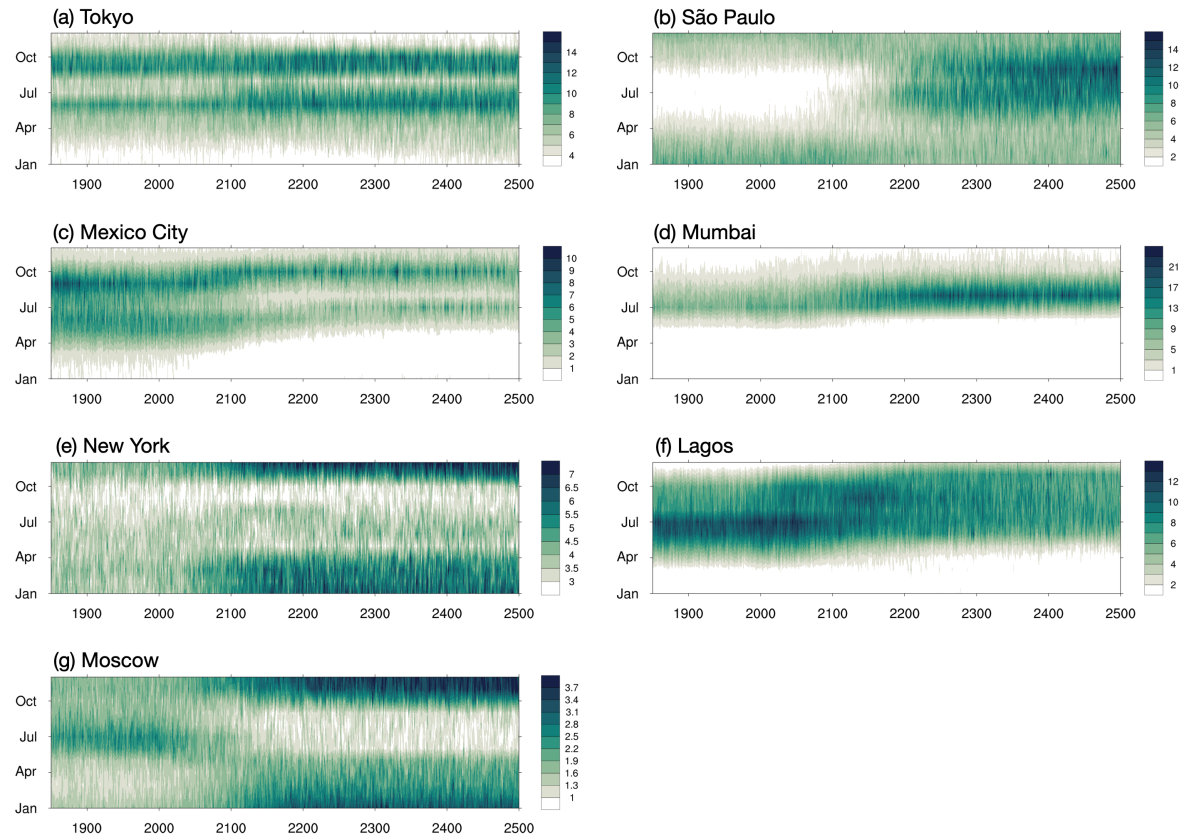

Figure S3: Monthly precipitation (mm day^{-1}) in (a) Tokyo (139.7°E, 35.7°N), (b) São Paulo (313.4°E, 23.6°S), (c) Mexico City (260.7°E, 19.4°N), (d) Mumbai (72.9°E, 19.1°N), (e) New York (286.0°E, 40.7°N), (f) Lagos (3.4°E, 6.5°N), and (g) Moscow (37.6°E, 55.8°N).

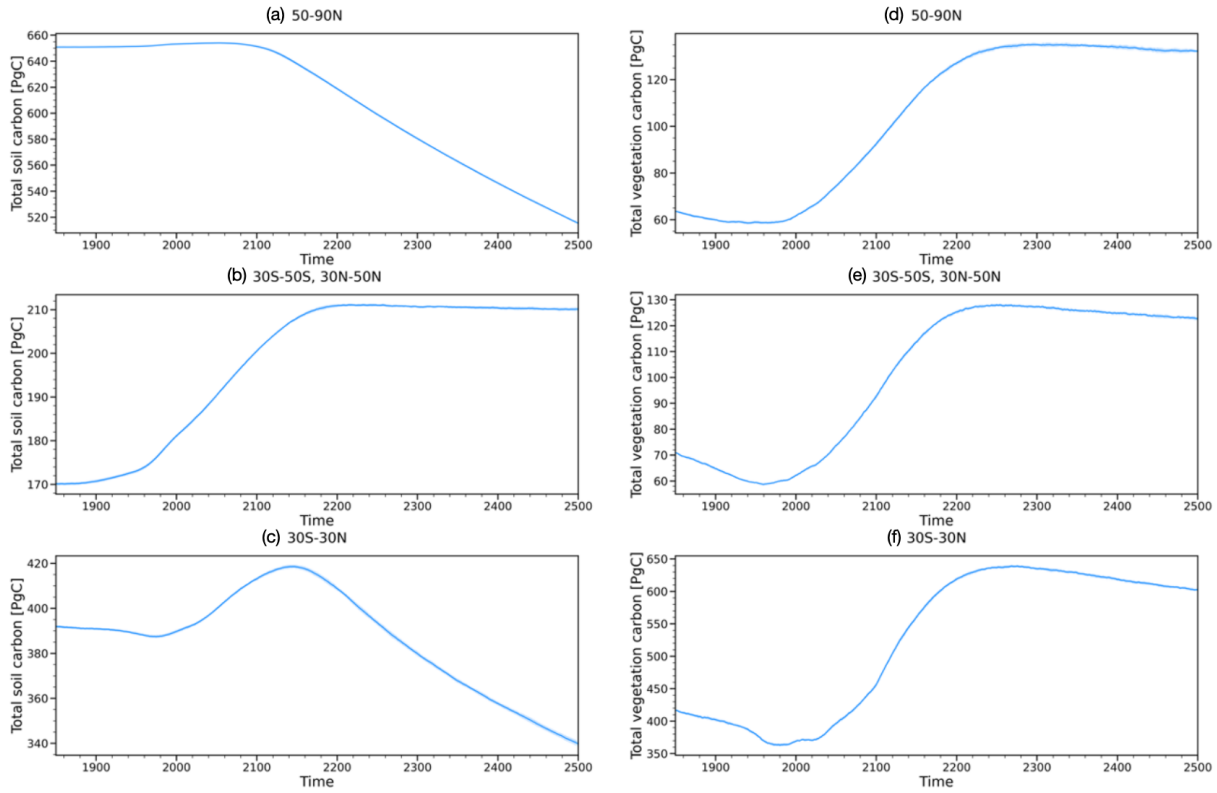

Figure S4: Time series of total soil carbon and total vegetation carbon. Total soil carbon (PgC) integrated over (a) 50°N-90°N, (b) 30°S-50°S and 30°N-50°N, and (c) 30°S-30°N. Total vegetation carbon (PgC) integrated over (d) 50°N-90°N, (e) 30°S-50°S and 30°N-50°N, and (f) 30°S-30°N.

Supplementary Table 1 Same as Table 1 except for integrated over 30°S-30°N.

30°S-30°N DIC PO_4	F_{100} (PgC yr^{-1}) ($TmolPO_4$ yr^{-1})	F_{1000} (PgC yr^{-1}) ($TmolPO_4$ yr^{-1})	Transfer efficiency	Mesopelagic Accumulation (Remineralization source) (PgC yr^{-1}) ($TmolPO_4$ yr^{-1})
1890s	3.971 2.534	0.602 0.394	0.152 0.155	3.369 2.141
1990s	3.927 (-1.1%) 2.520 (-0.6%)	0.612 (+1.7%) 0.398 (+1.1%)	0.156 0.158	3.315 (-1.6%) 2.122 (-13.4%)
2090s	3.809 (-4.1%) 2.240 (-11.6%)	0.644 (+7.0%) 0.391 (-0.6%)	0.169 0.175	3.165 (-6.1%) 1.849 (-13.6%)
2190s	2.968 (-25.3%) 1.642 (-35.2%)	0.529 (-12.1%) 0.300 (-23.9%)	0.178 0.182	2.439 (-27.6%) 1.342 (-37.3%)
2290s	2.555 (-35.7%) 1.393 (-45.0%)	0.472 (-21.6%) 0.262 (-33.4%)	0.185 0.188	2.083 (-38.2%) 1.131 (-47.2%)
2390s	2.334 (-41.2%) 1.288 (-49.2%)	0.445 (-26.2%) 0.245 (-37.8%)	0.188 0.190	1.890 (-43.9%) 1.043 (-51.3%)
2490s	2.256 (-43.2%) 1.221 (-51.8%)	0.424 (-29.5%) 0.233 (-40.8%)	0.188 0.191	1.832 (-45.6%) 0.988 (-53.8%)

Supplementary Table 2 Same as Table 1 except for integrated over 90°S-60°S.

90°S-60°S DIC PO_4	F_{100} (PgC yr^{-1}) ($TmolPO_4$ yr^{-1})	F_{1000} (PgC yr^{-1}) ($TmolPO_4$ yr^{-1})	Transfer efficiency	Mesopelagic Accumulation (Remineralization source) (PgC yr^{-1}) ($TmolPO_4$ yr^{-1})
1890s	0.1653 0.1177	0.0149 0.0106	0.0900 0.0901	0.1504 0.1071
1990s	0.1871 (+13.2%) 0.1332 (+13.0%)	0.0167 (+14.1%) 0.0121 (+14.1%)	0.0908 0.0908	0.1701 (+13.1%) 0.1211 (+13.1%)
2090s	0.2423 (+46.6%) 0.1726 (+46.6%)	0.0228 (+53.5%) 0.0163 (+53.5%)	0.0943 0.0943	0.2195 (+45.9%) 0.1563 (+45.9%)
2190s	0.3061 (+85.2%) 0.2179 (+85.1%)	0.0336 (+125.5%) 0.0205 (+93.7%)	0.1096 0.0942	0.2773 (+84.4%) 0.1974 (+84.3%)
2290s	0.3687 (+123.0%) 0.2625 (+123.0%)	0.0336 (+125.5%) 0.0239 (+125.5%)	0.0910 0.0910	0.3351 (+122.8%) 0.2386 (+122.8%)
2390s	0.3906 (+136.3%) 0.2780 (+136.0%)	0.0351 (+135.7%) 0.0250 (+135.7%)	0.0898 0.0899	0.3555 (+136.4%) 0.2530 (+136.2%)
2490s	0.3980 (+140.8%) 0.2833 (+140.7%)	0.0354 (+138.2%) 0.0252 (+138.1%)	0.0890 0.0891	0.3627 (+141.2%) 0.2581 (+141.0%)

Supplementary Table 3 The centennial-timescale ensemble-mean export ratio ($E_{F100/NPP}$), given as the ratio of export at 100 m (F_{100}) to depth-integrated NPP. For each variable, averages are conducted over 10 years, and changes relative to the 1890s are given in parentheses.

Export Ratio [$E_{F100/NPP}$] F_{100} (PgC yr^{-1}) NPP (PgC yr^{-1})	Global integral	30°S-30°N integral	90°S-30°S integral	30°N-90°N integral
1890s	**0.145** 6.98 48.3	**0.129** 3.97 30.7	**0.167** 1.70 10.2	**0.178** 1.32 7.4
1990s	**0.145 (+0.0%)** 7.08 (+1.4%) 48.8 (+1.0%)	**0.129 (+0.0%)** 3.98 (+0.2%) 30.8 (+0.3%)	**0.168 (+0.6%)** 1.76 (+3.8%) 10.5 (+2.9%)	**0.176 (-1.1%)** 1.34 (+1.7%) 7.6 (+2.7%)
2090s	**0.139 (-4.1%)** 6.91 (-1.0%) 49.8 (+3.1%)	**0.122 (-5.4%)** 3.81 (-4.1%) 31.3 (+2.0%)	**0.172 (+3.0%)** 2.00 (+17.6%) 11.6 (+13.7%)	**0.159 (-10.7%)** 1.10 (-16.5%) 6.9 (-6.7%)
2190s	**0.127 (-12.4%)** 5.85 (-16.2%) 46.1 (-4.6%)	**0.107 (-17.0%)** 2.97 (-25.2%) 27.8 (-9.4%)	**0.166 (-0.6%)** 2.07 (+21.8%) 12.5 (+22.5%)	**0.141 (-20.8%)** 0.82 (-37.9%) 5.8 (-21.6%)
2290s	**0.124 (-14.5%)** 5.43 (-22.2%) 43.9 (-9.1%)	**0.101 (-21.7%)** 2.55 (-35.7%) 25.2 (-17.9%)	**0.163 (-2.4%)** 2.13 (+25.5%) 13.1 (+28.4%)	**0.132 (-25.8%)** 0.74 (-43.7%) 5.6 (-24.3%)
2390s	**0.122 (-15.9%)** 5.21 (-25.4%) 42.6 (-11.8%)	**0.099 (-23.3%)** 2.37 (-40.2%) 24.0 (-21.8%)	**0.161 (-3.6%)** 2.14 (+25.9%) 13.3 (+30.4%)	**0.129 (-27.5%)** 0.69 (-47.3%) 5.4 (-27.0%)
2490s	**0.121 (-16.6%)** 5.06 (-27.6%) 41.7 (-13.7%)	**0.098 (-24.0%)** 2.26 (-43.2%) 23.1 (-24.8%)	**0.159 (-4.8%)** 2.13 (+25.3%) 13.4 (+31.4%)	**0.128 (-28.1%)** 0.67 (-49.3%) 5.2 (-29.7%)